

1 **Genomic sequencing of *Phyllosticta citriasiiana* provide insight into its**
2 **conservation and diversification with closely related *Phyllosticta***
3 **species associated with citrus**

4 Mingshuang Wang^{1, *}, Bei Liu², Ruoxin Ruan², Yibing Zeng², Jinshui Luo³, and
5 Hongye Li^{2, *}

6 ¹College of Life and Environmental Sciences, Hangzhou Normal University,
7 Hangzhou 310036, China

8 ²Key Lab of Molecular Biology of Crop Pathogens and Insects, Ministry of
9 Agriculture, and Institute of Biotechnology, Zhejiang University, Hangzhou 310058,
10 China

11 ³Fujian Institute of Tropical Crops, Zhangzhou 363001, China

12 *Authors for Correspondence: E-mails: mswang@hznu.edu.cn (M. Wang),
13 hyli@zju.edu.cn (H. Li)

14

15

16

17

18 **Abstract**

19 *Phyllosticta citriasiiana* is the causal agent of the pomelo tan spot. Here, we
20 presented the ~34Mb genome of *P. citriasiiana*. The genome is organized in 92
21 contigs, encompassing 9202 predicted genes. Comparative genomic analyses with
22 other two *Phyllosticta* species (*P. citricarpa* and *P. capitalensis*) associated with citrus
23 was conducted to understand their evolutionary conservation and diversification. Pair-
24 wise genome alignments revealed that these species are highly syntenic. All species
25 encode similar numbers of CAZymes and secreted proteins. However, the molecular
26 functions of the secretome showed that each species contains some enzymes with
27 distinct activities. Three *Phyllosticta* species shared a core set of 7261 protein
28 families. *P. capitalensis* had the largest set of orphan genes (2040), in complete
29 contrast to that of *P. citriasiiana* (371) and *P. citricarpa* (262). Most of the orphan
30 genes were functionally unknown, but they contain a certain number of species-
31 specific secreted proteins. A total of 23 secondary metabolites (SM) biosynthesis
32 clusters were identified in the three *Phyllosticta* species, 21 of them are highly
33 conserved among these species while the remaining 2 showed whole cluster gain and
34 loss polymorphisms or gene content polymorphisms. Taken together, our study
35 reveals insights into the genetic mechanisms of host adaptation of *Phyllosticta* species
36 associated with citrus and paves the way to identify effectors that function in infection
37 of citrus plants.

38

39 **Key words:** *Phyllosticta citriasiiana*; Pomelo tan spot; Comparative genomics;
40 Secreted proteins; Secondary metabolism

41

42

43 **Introduction**

44 Citrus Black Spot (CBS), caused by *Phyllosticta citricarpa*, is an important disease
45 of citrus, it can affect almost all grown citrus cultivars, including sweet orange (*Citrus*
46 *sinensis*), mandarin (*C. reticulata* and *C. unshiu*), pomelo (*C. maxima*), grapefruit (*C.*
47 *paradise*) and lemon (*C. limon*) (Wang et al., 2012). This disease mainly causes black
48 lesions in the fruits, making the fruits unsuitable for the fresh market. When the disease
49 is severe, yield losses are significant due to premature fruit drop (Kotzé, 1981). CBS
50 mainly happened in humid subtropical regions, including Asia, Africa, South America,
51 Australia, and most recently, Florida (Kotzé, 1981; Wang et al., 2012; Miles et al., 2013;
52 Wang et al., 2016b; Carstens et al., 2017). As this disease is previously absent in
53 Mediterranean countries like Spain, Italy, Israel, and Turkey, *P. citricarpa* was listed as
54 an A1 quarantine pest by European Union (Paul et al., 2005; EFSA, 2014). However, a
55 recent survey reported the presence of *P. citricarpa* in Italy, Malta and Portugal
56 (Guarnaccia et al., 2017).

57 Besides *P. citricarpa*, other species of *Phyllosticta* have been reported to be
58 associated with citrus. *P. citriasianna*, first identified to be a harmful pathogen of
59 pomelos in 2009, was able to cause necrotic spots (tan spots) on fruit similar to those
60 caused by *P. citricarpa* (Wulandari et al., 2009). By performing multi-locus
61 phylogenetic analyses on a large number of *Phyllosticta* species collected in China,
62 Wang et al. (2012) found that *P. citriasianna* was isolated only from pomelos, and *P.*
63 *citricarpa* was isolated from lemons, mandarins, and oranges, but never from pomelos,
64 indicating that the citrus-associated pathogenic *Phyllosticta* population may have a
65 host-related differentiation (Wang et al., 2012). In addition to *P. citriasianna*, many other
66 *Phyllosticta* fungi were also found in citrus, such as *P. capitalensis*, *P. citribraziliensis*,
67 *P. citrichinaensis*, *P. paracapitalensis*, and *P. paracitricarpa* (Glienke et al., 2011; Wang
68 et al., 2012; Guarnaccia et al., 2017). Of them, *P. capitalensis* is the most frequently
69 isolated species. This species has a very wide distribution and it has been isolated as
70 endophytes from dozens of plants (Wikee et al., 2013).

71 Due to the early discovery of *P. citricarpa* causing CBS and its economic

72 importance, *P. citricarpa* is extensively studied and many information is now available
73 on this pathogen's population structure, reproduction mode and introduction pathways
74 (Spósito et al., 2011; Wang et al., 2016b; Carstens et al., 2017). However, little is known
75 about the newly identified pathogen of pomelo tan spot, *P. citriasianna*. In this study, we
76 sequenced the genome of *P. citriasianna*, generating a high-quality reference genome
77 assembly and provide an overview of the genome structure of this important pathogen;
78 we also compared its genome with other two closely related *Phyllosticta* species
79 associated with citrus, i.e., *P. citricarpa* and *P. capitalensis* to provide insight into their
80 evolutionary conservation and diversification.

81

82 **Materials and Methods**

83 **Fungal strain**

84 The *Phyllosticta citriasianna* strain ZJUCC200914 (CGMCC3.14344) was isolated
85 from tan spot infected pomelos collected from Fujian Province, China (Wang et al.,
86 2012). Cultures of strains were maintained on regular solid PDA (potato dextrose agar)
87 or in liquid potato dextrose broth (PDB) at 25°C.

88 **Genome assembly and annotation**

89 The genomic DNA and RNA of *P. citriasianna* were extracted from mycelia grown
90 in PDB as described previously (Wang et al., 2015). The genome was first surveyed
91 through Illumina HiSeq 2500 platform using TruSeq libraries (150bp paired-end reads,
92 insert size of 350bp) and then sequenced using the long reads PacBio technology. A
93 total of 1.9 Gb PacBio data, 6.7 Gb pair-end data were generated in the sequencing
94 process, which corresponds to ~250 fold of sequence depth. To obtain high-quality gene
95 calls, RNA-Seq was conducted with the same sample and 6.0Gb Illumina paired-end
96 reads were obtained.

97 To obtain the *P. citriasianna* genome, the PacBio reads were initially assembled
98 using Canu 1.7 (Koren et al., 2017) and error correction was conducted using Pilon
99 version 1.22 with the Illumina reads (Walker et al., 2014). Genome quality assessment

100 was performed through the presence of conserved single-copy fungal genes using
101 BUSCO version 3 (Simao et al., 2015). RNA-seq data were aligned to the genome using
102 Bowtie 2.3.4 and TopHat 2.0.9 (Langmead and Salzberg, 2012; Kim et al., 2013).
103 Genome annotation was performed using the BRAKER version 1.0 pipeline combining
104 the RNA-seq-based gene prediction and ab initio gene prediction (Hoff et al., 2015).

105 The genomes of *P. citricarpa* (accession number LOEO00000000.1) and *P.*
106 *capitalensis* (accession number LOEN00000000.1) were downloaded from the NCBI
107 genome database (Wang et al., 2016b). Gene model predictions of these two genomes
108 were generated with AUGUSTUS 3.1 using the training annotation file of *Phyllosticta*
109 *citriasiiana* (Stanke et al., 2008). Repetitive elements were annotated in all assemblies
110 using RepeatMasker version open-4.0.7 (<http://www.repeatmasker.org>). For pairwise
111 syntenic analysis of genome structures, the contigs of the paired genomes of
112 *Phyllosticta* species were aligned with the MUMmer 3.23 package (Delcher et al.,
113 2003). The average nucleotide identity was estimated using the ANI calculator
114 (Rodriguez-R and Konstantinidis, 2016). The statistical reports for genomes were
115 calculated by using in-house Perl scripts.

116 **Functional annotation of genes.**

117 To functionally annotate gene models, we assigned protein sequence motifs to
118 protein families (Pfam) and gene ontology (GO) terms using the Pfam and eggNOG
119 databases (Huerta-Cepas et al., 2017; El-Gebali et al., 2018). The GO enrichment in
120 molecular functions was produced with the dcGO database (Fang and Gough, 2013).
121 Protein orthogroups were clustered using the orthoMCL algorithm in combination with
122 an all-versus-all protein BLAST search (e-value < 1e-10, identity > 50%) (Chen et al.,
123 2006). The carbohydrate-active enzymes were annotated by the web-based dbCAN2
124 meta server (Zhang et al., 2018). To identify secreted proteins, we use SingalP 4.1 to
125 predict the transmembrane domains and we excluded non-extracellular and GPI-
126 anchored proteins by using targetP 1.1 (Emanuelsson et al., 2000) and GPI-SOM
127 (Fankhauser and Mäser, 2005). Fungal secondary metabolite pathways were predicted
128 using the online tool antiSMASH 4.0 (Blin et al., 2017).

129 **Data availability:** The assembled *Phyllosticta citriasiiana* genome has been deposited
130 in GenBank under the accession number QOCM00000000. All the annotation data
131 generated in this study have been deposited on the figshare repository at DOI:
132 10.6084/m9.figshare.9178061 (the data will be made publicly available upon
133 acceptance of the manuscript).

134

135 **Results and discussion**

136 **Genome assembly and general features**

137 We assembled the genome of *P. citriasiiana* using a combination of Illumina and
138 PacBio reads with ~250 fold of sequence depth. The de novo assembly resulted in a
139 genome size of 34.2 Mb assembled in 92 contigs with an N50 of ~1Mb. The genomes
140 of *P. citricarpa* and *P. capitalensis* previously sequenced were utilized and annotated in
141 this study (Wang et al., 2016b). The completeness of these three genome assemblies
142 was estimated by BUSCO (Simao et al., 2015). We found 1759 out of 1732 (98.4%)
143 BUSCO groups were identified in the *P. citriasiiana* genome, indicating a high degree
144 of completeness. Although the assembly of *P. citricarpa* and *P. capitalensis* possess a
145 large number of contigs, the BUSCO results showed that they are around 95%
146 completeness, suggesting that these genomes are reliable for the downstream analyses
147 (Table 1).

148 The overall G + C content of *P. citriasiiana* (51.4%) is apparently lower than that
149 of *P. citricarpa* (53.1%) and *P. capitalensis* (54.6%). The percentage of repetitive
150 sequences of *P. citriasiiana* is 2.19%, around 2-fold of that of *P. citricarpa* (0.97%) and
151 7-fold of *P. capitalensis* (0.29%). *P. citriasiiana* has the lowest gene density but the
152 longest gene length among the three species. The genome of *P. citriasiiana* was
153 predicted to have 9202 proteins, which is comparable with that of *P. citricarpa* (9083),
154 but much lower than that (9983) of *P. capitalensis* genome (Table 1).

155 During preparing this manuscript, we noticed that a paper describing the genomic

156 sequencing of *P. citricarpa* and *P. capitalensis* was published (Rodrigues et al., 2019).
157 However, the general features of their genome sequences are of great difference from
158 ours. For example, the authors predicted ~15000 proteins for both species while our
159 data only predicted ~9500 ones. In that study, we found that the *P. citricarpa* genomic
160 assembly consisted of 19,143 contigs with the N50 of 3049bp and the *P. capitalensis*
161 genomic assembly contains 11,080 contigs with the N50 of 4925bp (Rodrigues et al.,
162 2019). This means that their genome sequence was very fragmented and the
163 incompleteness of the genome was also confirmed by their BUSCO analysis (Rodrigues
164 et al., 2019). Thus, comparing with their genomic data, we believe that the data in this
165 study is much better and more reliable.

166

167 **Genomic similarity**

168 The pairwise comparison analysis based on oriented contigs reveals a high degree
169 of genome-wide macrosynteny between *P. citriasiiana* and the other two species (Fig.
170 1A). However, the average nucleotide identity (95.98%) between *P. citriasiiana* and *P.*
171 *citricarpa* is much larger than that (81.19%) between *P. citriasiiana* and *P. capitalensis*
172 (Fig. 1B), indicating that *P. citriasiiana* is much closer to *P. citricarpa* and relatively far
173 from *P. capitalensis*.

174 **Carbohydrate active enzymes and secretomes**

175 The cell wall in plant forms a complex network of different polysaccharides that
176 includes cellulose, hemicellulose, pectin, and lignin. Carbohydrate-active enzymes
177 (CAZymes) play important roles in the breakdown of complex carbohydrates and are
178 responsible for the acquisition of nutrients from the plant for plant-associated fungi
179 (Kubicek et al., 2014). A total of 183 putative CAZyme genes were identified in *P.*
180 *citriasiiana*, which includes 100 Glycoside Hydrolases (GHs), 46 Glycosyl Transferases
181 (GTs), 30 Auxiliary Activities (AAs), 3 Carbohydrate Esterases (CEs), 3
182 Polysaccharide Lyases (PLs), and 1 Carbohydrate-Binding Modules (CBMs) (Table S1-
183 4). The types and numbers of CAZymes among different species of *Phyllosticta* are

184 very similar (Table S1-4). When compared with other species in the Dothideomycetes,
185 *P. citriasiiana* appears to contain a much less extensive set of CAZymes, for example,
186 *Alternaria alternata* has 373 CAZymes while *Zymoseptoria tritici* contains 324 ones
187 (Goodwin et al., 2011; Ohm et al., 2012; Wang et al., 2016a). The smaller number of
188 CAZymes in *Phyllosticta* coincides with the phenomenon that these species have a
189 relatively long time to infect citrus fruits and the scab expanded slowly in the fruit peels
190 (Wang et al., 2012; Goulin et al., 2016).

191 Pathogens can secrete a series of proteins that are deployed to the host-pathogen
192 interface during infection, and secretome proteins play an important role in
193 pathogenicity (Presti et al., 2015). Approximately 5% of the total proteins (470) of *P.*
194 *citriasiiana* are predicted to be secreted (Table S5-8). ‘Hydrolase activity’ was the most
195 abundant molecular function of the secretome, other GO terms over-represented among
196 the secreted proteins include ‘hydrolase activity, acting on glycosyl bonds’, ‘carboxylic
197 ester hydrolase activity’, ‘lipase activity’, ‘exopeptidase activity’, ‘serine hydrolase
198 activity’, and ‘hydrolase activity, acting on carbon-nitrogen bonds’ (Table 2). The other
199 two *Phyllosticta* species contain a similar number of SPs with *P. citriasiiana*, i.e., 465
200 in *P. citricarpa* and 491 in *P. capitalensis* (Table S5-8). However, their GO categories
201 showed some differences from that of *P. citriasiiana*. The SPs of *P. citricarpa* were not
202 enriched in ‘exopeptidase activity’, ‘serine hydrolase activity’, and ‘hydrolase activity,
203 acting on carbon-nitrogen bonds’ but was in ‘transferase activity, transferring hexosyl
204 groups’ (Table 2). The SPs of *P. capitalensis* lacks ‘exopeptidase activity’ and
205 ‘hydrolase activity, acting on carbon-nitrogen bonds’ but contains ‘phosphatase
206 activity’, ‘transferase activity, transferring hexosyl groups’, and ‘UDP-
207 glycosyltransferase activity’ (Table 2). These results suggested that the constitution of
208 different *Phyllosticta* secretomes has changed, each species have some preferred
209 enzymes with distinct activities.

210 **Orthologs groups and orphan genes**

211 We then searched the conservation and diversification of proteins among different
212 *Phyllosticta* species from genome-scale. The protein orthology analysis identified 7261

213 orthologous groups existed in all the three *Phyllosticta* species, constituting the core
214 gene set of *Phyllosticta* (Fig. 2). To find if any protein might be under positive selection,
215 the dN/dS ratios for predicted proteins in a pairwise comparison between *P. citriasianna*
216 and the other two *Phyllosticta* species were calculated. However, all gene show signs
217 of purifying selection (dN/dS<1). 2040 genes in *P. capitalensis* have no orthologs in the
218 other two species (Fig. 2), suggesting that these genes might play roles in constructing
219 the endophytic relationship of *P. capitalensis* with its host. *P. citriasianna* and *P.*
220 *citricarpa* encoded 371 and 262 species-specific proteins, respectively (Fig. 2),
221 suggesting that these genes might be related to the host-specific pathogenicity. To know
222 the functions of the genes in those three gene sets, we annotated them using the
223 eggNOG database. However, the results showed that the majority of genes in each
224 group encoded proteins without well-characterized domains and very few sequences
225 can be assigned to the GO terms (Table S9-12).

226 We are then curious about if the distribution of CAZymes and secreted proteins
227 might differ among different gene sets. We found that the *P. capitalensis* orphan genes
228 contain only one CAZyme gene which encodes the AA3 family of cellobiose
229 dehydrogenase while the other two species' orphan genes contain no CAZyme gene
230 (Table S13). However, the case for the secreted proteins is much different. *P.*
231 *capitalensis*, *P. citricarpa*, and *P. citriasianna* contain 75, 8 and 17 species-specific
232 secreted proteins, respectively (Table S13). These results indicate that *Phyllosticta*
233 species have formed lineage-specific sets of orphan genes which might have a potential
234 role in species diversification. Although functions of most orphans are unknown, the
235 secreted proteins (potential effectors) are likely the essential factors of host
236 specialization and they might be good candidates for future functional characterization
237 in distinct *Phyllosticta* species.

238 Secondary metabolite gene clusters

239 We identified 23 secondary metabolites (SM) biosynthesis clusters in the three
240 *Phyllosticta* species (Table S14). These clusters are comprised of 3 NRPS clusters, 5
241 PKS clusters, 4 terpene clusters, 1 terpene-NRPS cluster, 1 PKS-NRPS cluster, and 9

242 clusters do not fit into any category (Table S14). Of them, cluster C9 contains all
243 *Alternaria solani* genes involved in alternapyrone synthesis, suggesting that these
244 *Phyllosticta* species have the potential to synthesize alternapyrone or its derivatives
245 (Fujii et al., 2005). Most SM clusters (21) are well conserved among the three
246 *Phyllosticta* species while 2 SM clusters of them showed whole cluster gain and loss
247 polymorphisms or gene content polymorphisms. Cluster C7 was present in *P. citricarpa*
248 and *P. citriasiiana* but absent from *P. capitalensis*, indicating that this cluster might be
249 lost in *P. capitalensis* or gained in the common ancestor of *P. citricarpa* and *P.*
250 *citriasiiana*. Meanwhile, Cluster C7 in *P. citricarpa* possesses another 3 genes while *P.*
251 *citriasiiana* contains a ~11 Kb region encoding no proteins, showing gene content
252 polymorphisms (Fig. 3). SM cluster C23 showed two gene content polymorphisms. One
253 is that the *P. capitalensis* has an additional 4 genes between orthologous gene OG0649
254 and OG0648. The other is *P. citriasiiana* lost two genes, of which gene OG7537 encodes
255 the backbone of this cluster (Fig. 3). A following tBLASTn analysis against the *P.*
256 *citriasiiana* genome confirmed the loss of these two genes. This gene content
257 polymorphism was most likely generated through a genomic deletion event, rendering
258 the SM gene cluster nonfunctional.

259 Secondary metabolites, especial fungal toxins, are believed to be involved in the
260 pathogenicity of many plant pathogenic fungal species and can be described as potential
261 virulence factors. Previously, a handful of secondary metabolites from the citrus
262 pathogen *P. citricarpa* were identified and characterized. Of them, a new dioxolanone,
263 phenguignardic acid butyl ester, showed low phytotoxic activity in citrus leaves and
264 fruits (at a dose of 100 µg) (Savi et al., 2019). However, the involvement of this
265 compound in the formation of citrus black spot disease needs to be further addressed.
266 In this study, we observed the major structural variation of two SM clusters among
267 different *Phyllosticta* species, therefore, distinct corresponding metabolites are
268 expected. However, if they are involved in the host specialization are not known. So,
269 future investigations and elucidations of secondary metabolic mechanisms in
270 *Phyllosticta* species and their functions involved in plant-fungal interactions will be of

271 great significance.

272

273 **Conclusions**

274 In this study, we sequenced the genome of *P. citriásiana*, the causal agent of the
275 pomelo tan spot, generating a high-quality reference genome assembly and provide an
276 overview of the genome structure of this important pathogen. We performed
277 comparative genomics analysis to reveal overall high similarities in sequence identity
278 and gene content among *P. citriásiana*, *P. citricarpa*, and *P. capitalensis*, reflecting the
279 phylogenetic and ecological relatedness of these species associated with citrus. Our data
280 also highlighted several striking differences in the constitution of secretomes, species-
281 specific genes, and secondary metabolite gene clusters, which might contribute to the
282 formation of fungal diversity. However, it is yet to be determined how a *Phyllosticta*
283 species emerged as a pathogen of alternate hosts. These data would be valuable in the
284 future investigation of the driving forces of fungal host switch, in population genomic
285 studies for identification of haplotypes and alleles, and in identifying effectors that may
286 function in infection of citrus plants.

287

288 **Author Contributions**

289 MW and HL conceived the study. All authors analyzed the data. MW wrote the paper.
290 All authors reviewed the manuscript.

291

292 **Fundings**

293 This study was supported by National key research and development program
294 (2017YFD0202000), the China Agriculture Research System (CARS-26) and Basic
295 special funds for public welfare research institutes in Fujian Province (2019R1010-4).

296

297 **Conflict of Interest Statement**

298 The authors declare no competing financial interests.

299

300 **Literature Cited**

301 Blin, K., Wolf, T., Chevrette, M.G., Lu, X., Schwalen, C.J., Kautsar, S.A., et al. (2017). antiSMASH 4.0-
302 improvements in chemistry prediction and gene cluster boundary identification. *Nucleic Acids
303 Res* 28(10).

304 Carstens, E., Linde, C., Slabbert, R., Miles, A., Donovan, N., Li, H., et al. (2017). A global perspective
305 on the population structure and reproductive system of *Phyllosticta citricarpa*. *Phytopathology*
306 107(6), 758-768.

307 Chen, F., Mackey, A.J., Stoeckert, C.J., Jr., and Roos, D.S. (2006). OrthoMCL-DB: querying a
308 comprehensive multi-species collection of ortholog groups. *Nucleic Acids Res* 34(Database
309 issue), D363-368.

310 Delcher, A.L., Salzberg, S.L., and Phillippy, A.M. (2003). Using MUMmer to identify similar regions in
311 large sequence sets. *Curr Protoc Bioinformatics* 10(10).

312 EFSA (2014). Scientific opinion on the risk of *Phyllosticta citricarpa* (*Guignardia citricarpa*) for the EU
313 territory with identification and evaluation of risk reduction options. *EFSA Journal* 12(2), 3557.

314 El-Gebali, S., Mistry, J., Bateman, A., Eddy, S.R., Luciani, A., Potter, S.C., et al. (2018). The Pfam protein
315 families database in 2019. *Nucleic Acids Research* 47(D1), D427-D432.

316 Emanuelsson, O., Nielsen, H., Brunak, S., and Von Heijne, G. (2000). Predicting subcellular localization
317 of proteins based on their N-terminal amino acid sequence. *Journal of Molecular Biology* 300(4),
318 1005-1016.

319 Fang, H., and Gough, J. (2013). DcGO: database of domain-centric ontologies on functions, phenotypes,
320 diseases and more. *Nucleic Acids Res* 41(Database issue), D536-544. doi: 10.1093/nar/gks1080.

321 Fankhauser, N., and Mäser, P. (2005). Identification of GPI anchor attachment signals by a Kohonen self-
322 organizing map. *Bioinformatics* 21(9), 1846-1852.

323 Fujii, I., Yoshida, N., Shimomaki, S., Oikawa, H., and Ebizuka, Y. (2005). An iterative type I polyketide
324 synthase PKSN catalyzes synthesis of the decaketide alternapryrone with regio-specific octa-
325 methylation. *Chemistry & Biology* 12(12), 1301-1309.

326 Glienke, C., Pereira, O.L., Stringari, D., Fabris, J., Kava-Cordeiro, V., Galli-Terasawa, L., et al. (2011).
327 Endophytic and pathogenic *Phyllosticta* species, with reference to those associated with Citrus
328 Black Spot. *Persoonia* 26, 47-56.

329 Goodwin, S.B., M'barek, S.B., Dhillon, B., Wittenberg, A.H., Crane, C.F., Hane, J.K., et al. (2011).
330 Finished genome of the fungal wheat pathogen *Mycosphaerella graminicola* reveals dispensome
331 structure, chromosome plasticity, and stealth pathogenesis. *PLoS Genet* 7(6), e1002070.

332 Goulin, E.H., Savi, D.C., Petters, D.A.L., Kava, V., Galli-Terasawa, L., Silva, G.J., et al. (2016).
333 Identification of genes associated with asexual reproduction in *Phyllosticta citricarpa* mutants
334 obtained through *Agrobacterium tumefaciens* transformation. *Microbiological Research* 192,

335 142-147. doi: <https://doi.org/10.1016/j.micres.2016.06.010>.

336 Guarnaccia, V., Groenewald, J.Z., Li, H., Glienke, C., Carstens, E., Hattingh, V., et al. (2017). First report
337 of *Phyllosticta citricarpa* and description of two new species, *P. paracapitalensis* and
338 *P. paracitricarpa*, from citrus in Europe. *Studies in Mycology* 87, 161-185. doi:
339 <https://doi.org/10.1016/j.simyco.2017.05.003>.

340 Hoff, K.J., Lange, S., Lomsadze, A., Borodovsky, M., and Stanke, M. (2015). BRAKER1: unsupervised
341 RNA-Seq-based genome annotation with GeneMark-ET and AUGUSTUS. *Bioinformatics*
342 32(5), 767-769.

343 Huerta-Cepas, J., Forslund, K., Coelho, L.P., Szklarczyk, D., Jensen, L.J., von Mering, C., et al. (2017).
344 Fast genome-wide functional annotation through orthology assignment by eggNOG-mapper.
345 *Molecular Biology and Evolution* 34(8), 2115-2122.

346 Kim, D., Pertea, G., Trapnell, C., Pimentel, H., Kelley, R., and Salzberg, S.L. (2013). TopHat2: accurate
347 alignment of transcriptomes in the presence of insertions, deletions and gene fusions. *Genome
348 Biol* 14(4), 2013-2014.

349 Koren, S., Walenz, B.P., Berlin, K., Miller, J.R., Bergman, N.H., and Phillippy, A.M. (2017). Canu:
350 scalable and accurate long-read assembly via adaptive k-mer weighting and repeat separation.
351 *Genome Research* 27(5), 722-736.

352 Kotzé, J.M. (1981). Epidemiology and control of citrus black spot in south-Africa. *Plant Disease* 65(12),
353 945-950.

354 Kubicek, C.P., Starr, T.L., and Glass, N.L. (2014). Plant cell wall-degrading enzymes and their secretion
355 in plant-pathogenic fungi. *Annual Review of Phytopathology* 52, 427-451.

356 Langmead, B., and Salzberg, S.L. (2012). Fast gapped-read alignment with Bowtie 2. *Nature Methods*
357 9(4), 357-359.

358 Miles, A.K., Tan, Y.P., Tan, M.K., Donovan, N.J., and Ghalayini, A. (2013). *Phyllosticta* spp. on
359 cultivated Citrus in Australia. *Australasian Plant Pathology* 42(4), 461-467. doi:
360 [10.1007/s13131-013-0208-0](https://doi.org/10.1007/s13131-013-0208-0).

361 Ohm, R.A., Feau, N., Henrissat, B., Schoch, C.L., Horwitz, B.A., Barry, K.W., et al. (2012). Diverse
362 Lifestyles and Strategies of Plant Pathogenesis Encoded in the Genomes of Eighteen
363 Dothideomycetes Fungi. *PLoS Pathogens* 8(12), e1003037. doi: 10.1371/journal.ppat.1003037.

364 Paul, I., van Jaarsveld, A.S., Korsten, L., and Hattingh, V. (2005). The potential global geographical
365 distribution of Citrus Black Spot caused by *Guignardia citricarpa* (Kiely): likelihood of disease
366 establishment in the European Union. *Crop Protection* 24(4), 297-308. doi:
367 <https://doi.org/10.1016/j.cropro.2004.08.003>.

368 Presti, L.L., Lanver, D., Schweizer, G., Tanaka, S., Liang, L., Tollot, M., et al. (2015). Fungal Effectors
369 and Plant Susceptibility. *Annual Review of Plant Biology* 66(1), 513-545. doi: 10.1146/annurev-
370 arplant-043014-114623.

371 Rodrigues, C.M., Takita, M.A., Silva, N.V., Ribeiro-Alves, M., and Machado, M.A. (2019). Comparative
372 genome analysis of *Phyllosticta citricarpa* and *Phyllosticta capitalensis*, two fungi species that
373 share the same host. *BMC Genomics* 20(1), 554. doi: 10.1186/s12864-019-5911-y.

374 Rodriguez-R, L.M., and Konstantinidis, K.T. (2016). "The enveomics collection: a toolbox for
375 specialized analyses of microbial genomes and metagenomes". PeerJ Preprints).

376 Savi, D.C., Shaaban, K.A., Mitra, P., Ponomareva, L.V., Thorson, J.S., Glienke, C., et al. (2019).
377 Secondary metabolites produced by the citrus phytopathogen *Phyllosticta citricarpa*. *The
378 Journal of antibiotics* 72(5), 306.

379 Simao, F.A., Waterhouse, R.M., Ioannidis, P., Kriventseva, E.V., and Zdobnov, E.M. (2015). BUSCO:
380 assessing genome assembly and annotation completeness with single-copy orthologs.
381 *Bioinformatics* 31(19), 3210-3212.

382 Spósito, M.B., Amorim, L., Bassanezi, R.B., Yamamoto, P.T., Felippe, M.R., and Czermainski, A.B.C.
383 (2011). Relative importance of inoculum sources of *Guignardia citricarpa* on the citrus black
384 spot epidemic in Brazil. *Crop Protection* 30(12), 1546-1552.

385 Stanke, M., Diekhans, M., Baertsch, R., and Haussler, D. (2008). Using native and syntenically mapped
386 cDNA alignments to improve de novo gene finding. *Bioinformatics* 24(5), 637-644.

387 Walker, B.J., Abeel, T., Shea, T., Priest, M., Abouelliel, A., Sakthikumar, S., et al. (2014). Pilon: an
388 integrated tool for comprehensive microbial variant detection and genome assembly
389 improvement. *PLoS One* 9(11), e112963.

390 Wang, M., Sun, X., Yu, D., Xu, J., Chung, K., and Li, H. (2016a). Genomic and transcriptomic analyses
391 of the tangerine pathotype of *Alternaria alternata* in response to oxidative stress. *Sci Rep*
392 6(32437).

393 Wang, M., Sun, X., Zhu, C., Xu, Q., Ruan, R., Yu, D., et al. (2015). PdbrlA, PdabaA and PdwetA control
394 distinct stages of conidiogenesis in *Penicillium digitatum*. *Res Microbiol* 166(1), 56-65.

395 Wang, N.Y., Zhang, K., Huguet-Tapia, J.C., Rollins, J.A., and Dewdney, M.M. (2016b). Mating Type
396 and Simple Sequence Repeat Markers Indicate a Clonal Population of *Phyllosticta citricarpa* in
397 Florida. *Phytopathology* 106(11), 1300-1310.

398 Wang, X., Chen, G., Huang, F., Zhang, J., Hyde, K.D., and Li, H. (2012). *Phyllosticta* species associated
399 with citrus diseases in China. *Fungal Diversity* 52(1), 209-224.

400 Wikee, S., Lombard, L., Crous, P.W., Nakashima, C., Motohashi, K., Chukeatirote, E., et al. (2013).
401 *Phyllosticta capitalensis*, a widespread endophyte of plants. *Fungal Diversity* 60(1), 91-105. doi:
402 10.1007/s13225-013-0235-8.

403 Wulandari, N., To-Anun, C., Hyde, K., Duong, L., De Gruyter, J., Meffert, J., et al. (2009). *Phyllosticta*
404 *citriasiiana* sp. nov., the cause of Citrus tan spot of *Citrus maxima* in Asia. *Fungal Diversity*
405 34(1), 23-39.

406 Zhang, H., Yohe, T., Huang, L., Entwistle, S., Wu, P., Yang, Z., et al. (2018). dbCAN2: a meta server for
407 automated carbohydrate-active enzyme annotation. *Nucleic Acids Research* 46(W1), W95-
408 W101. doi: 10.1093/nar/gky418.

409

410

411

412

413
414
415
416

Table 1 Genomic features of three *Phyllosticta* species associated with citrus.

Features	<i>P. capitalensis</i> strain Gm33	<i>P. citricarpa</i> strain Gc12	<i>P. citriasihana</i> strain CGMCC3.14344
Genome size (Mb)	32.4	31.1	34.2
BUSCOs (%)	95.5	94.8	98.4
Number of contigs	1341	5748	92
N50 (Kb)	20.8	76	968.9
GC content (%)	54.6	53.1	51.4
Protein-coding genes	9983	9083	9202
Gene density (number of genes per Mb)	308	292	269
Mean gene length (bp)	1632	1642	1677
Repeat rate (%)	0.29	0.97	2.19

417

418

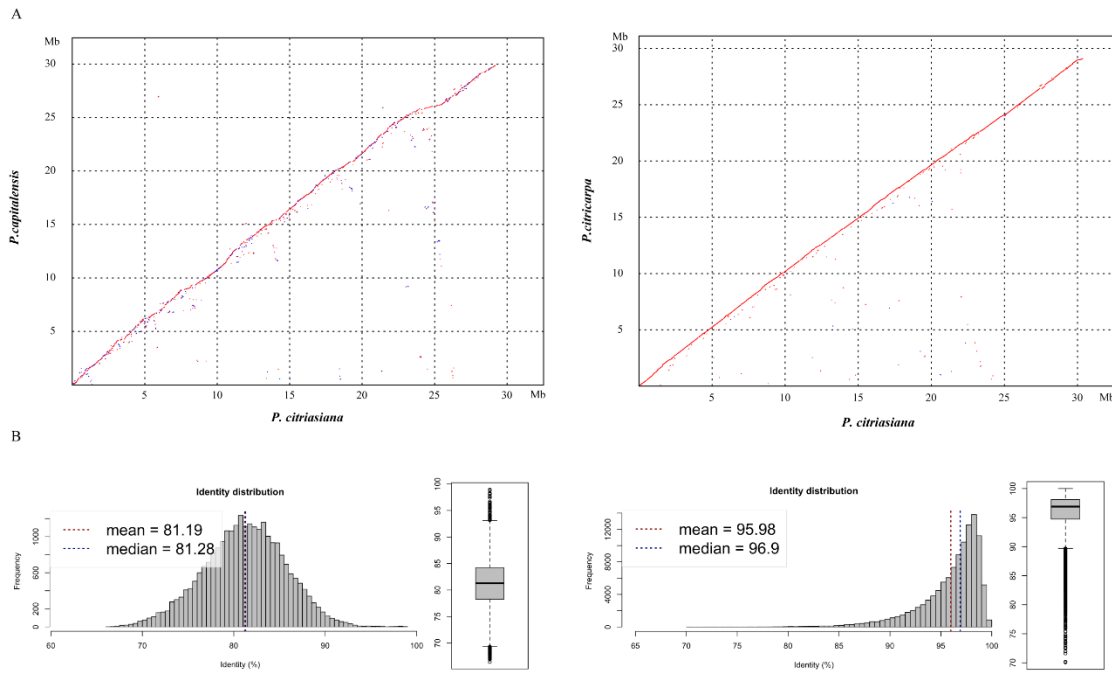
419

Table 2 Enriched molecular functional categories for secreted proteins genes of *Phyllosticta* species associated with citrus.

Species	GO id	GO term	FDR	Gene number
<i>P. citriasiana</i>	GO:0016787	hydrolase activity	2.82E-21	82
	GO:0016798	hydrolase activity, acting on glycosyl bonds	1.34E-19	29
	GO:0052689	carboxylic ester hydrolase activity	4.44E-07	12
	GO:0016298	lipase activity	3.61E-05	10
	GO:0008238	exopeptidase activity	8.67E-04	8
	GO:0017171	serine hydrolase activity	6.66E-03	7
<i>P. citricarpa</i>	GO:0016810	hydrolase activity, acting on carbon-nitrogen bonds	9.33E-03	8
	GO:0016787	hydrolase activity	4.80E-17	76
	GO:0016798	hydrolase activity, acting on glycosyl bonds	1.57E-20	30
	GO:0052689	carboxylic ester hydrolase activity	4.56E-06	11
	GO:0016298	lipase activity	2.10E-04	9
	GO:0016758	transferase activity, transferring hexosyl groups	2.42E-03	10
<i>P. capitalensis</i>	GO:0016787	hydrolase activity	1.48E-18	100
	GO:0016798	hydrolase activity, acting on glycosyl bonds	6.07E-15	29
	GO:0052689	carboxylic ester hydrolase activity	5.68E-08	15
	GO:0016298	lipase activity	1.76E-04	11
	GO:0016791	phosphatase activity	3.96E-04	13
	GO:0016758	transferase activity, transferring hexosyl groups	4.07E-04	14
	GO:0017171	serine hydrolase activity	1.14E-03	10
	GO:0008238	exopeptidase activity	1.90E-03	9
	GO:0008194	UDP-glycosyltransferase activity	6.87E-03	8

420

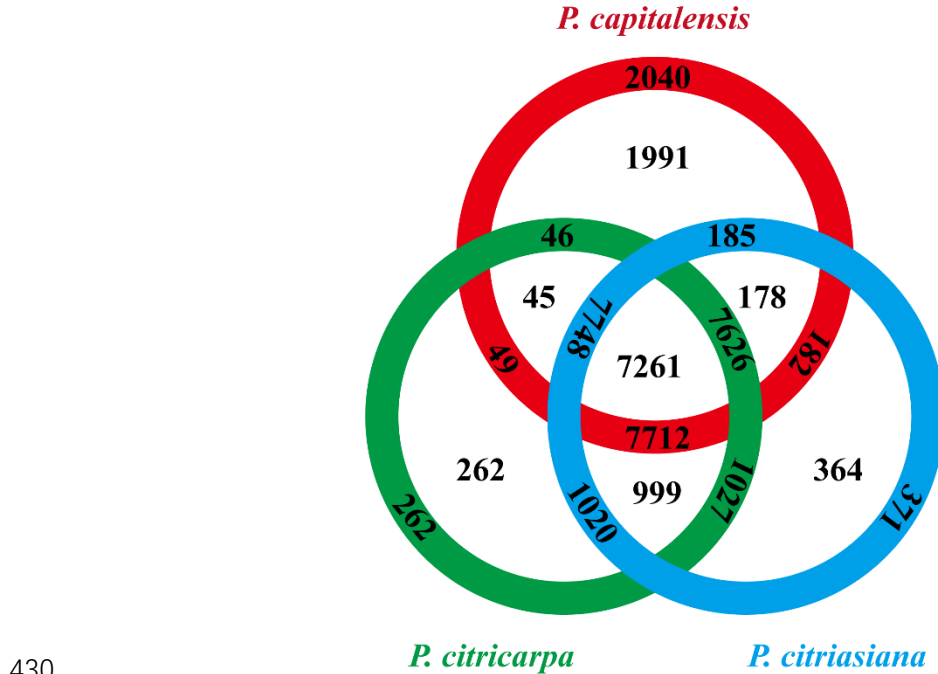
421 **Figure legends**



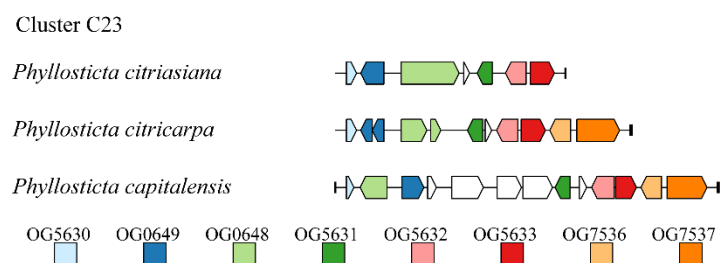
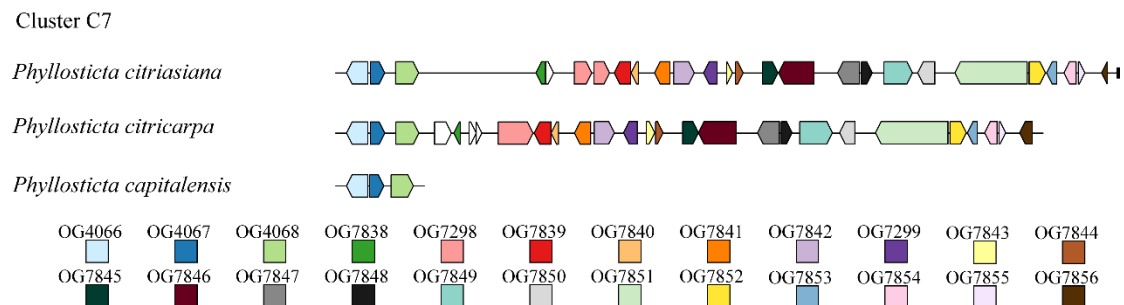
422

423 **Fig. 1** Genomic similarity between *P. citri asana* and the other two *Phyllosticta*
424 species (*P. citricarpa* and *P. capitalensis*) associated with citrus. **A**) Dotplots showing
425 genome nucleotide alignments of *P. citri asana* with *P. citricarpa* and *P. capitalensis*.
426 Red diagonals represent alignments in the same direction, whereas blue ones suggest
427 a reverse orientation. **B**) Distribution of nucleotide identities between *P. citri asana*
428 and the other two *Phyllosticta* species.

429



430
431 **Fig. 2** Numbers of orthologous groups that are unique to each isolate, specific to two
432 isolates, and common to all three *Phyllosticta* isolates. Corresponding gene numbers
433 are indicated in the outer ring.
434



435
436 **Fig. 3** Structural variations of secondary metabolic (SM) gene cluster C7 and C23
437 among *Phyllosticta* species associated with citrus. For each SM cluster, orthologues
438 among different species are marked with the same color. Genes marked by white lack
439 orthologues in other species. The short black vertical line indicates the end of the

440 contig.
441
442
443
444
445